# Minimizing Current Ripple in Three-Phase, Four Wire, Voltage Source Converters by the injection of an Optimal Zero Sequence Signal to a Triangular Carrier PWM

[1,2,3] Lourenço Matakas Júnior [1,4] Walter Pereira da Silva Júnior [1] Antônio Ricardo Giaretta
[1] Polytechnic School of the University of Sao Paulo - Departament of Energy and Automation
Av. Prof. Luciano Gualberto , trav.3, no. 158, cep:05508-900 – São Paulo – SP – Brazil: phone. + 55 (11) 3091-5623
[2] Pontifícia Universidade Católica de São Paulo [3] Universidade São Judas Tadeu [4] Fairchild Semiconductor
Matakas@pea.usp.br Walter.silva@poli.usp.br Antonio.giaretta@poli.usp.br

***Abstract*** **- This paper proposes a strategy for the minimization of the line and neutral ripple current of a three-phase four-wire, four poles, Voltage Source Converter. The strategy consists of injecting an instantaneous zero sequence to the references of a triangular carrier PWM that does not affects the local average of the converter output voltages, but only the ripple currents. A methodology to evaluate the instantaneous optimal value of the injected zero sequence voltage is presented. The locus of the synthesizable voltage vectors and the modeling of the converter are also presented. Experimental results are presented to validate the proposed approach.**

***Keywords*** **- Three-phase four-wire converter, Carrier-based PWM, Zero sequence injection.**

## I. INTRODUCTION

Three-Phase, Four Wire Voltage Source Converters (VSC3F4W) are used in low voltage UPS systems and Active Filters. There are two topologies for this converter. The first one (VSC3F4W-3L) uses a conventional three-phase converter with three switching poles, where the neutral point is obtained at the central point of the DC side capacitor. In the second one (VSC3F4W-4L), the neutral is obtained at the central point of an additional switching pole (figure 1). This second version is preferable in spite of its higher cost, for providing higher range at the AC output voltage for the same DC link voltage. Additionally there is the possibility of current ripple reduction by zero sequence injection at the PWM reference signals. Many papers have been presented about PWM generation for the VSI3F4W-FL [3,4,5,8,9,10,11,12]. Many of them prefer the Space Vector based strategies [3,4,8,10,11,12] because of its better DC link utilization and lower current ripple. Carrier based PWM are discussed in 5,8,9,11 without taking into account the ripple current.

This paper shows that the same performance of the Space Vector PWM can be achieved by injecting an optimal value of zero sequence signal $v_{0\_ref}$ to the four carrier based PWM blocks of the VSI3F4W-FL. The use of triangular carrier based PWM is justified by:

- its simplicity and good performance;
- its availability in DSPs and microcontrollers dedicated to "Motor Control" applications;
- the lower computational burden (the PWM generation is done by dedicated hardware at the processor chip);
- the results compiled in [1,2,4,6,7,14] for three phase, three wire converters, showing that the Space Vector behavior can be obtained by triangular carrier PWM with zero sequence injection.

Item II discusses the locus of the Space Vectors that can be synthesized by the VSC3F4W-4L. Item III presents the converter modeling. Item IV discusses the zero sequence injection in the carrier based PWM and its effect on current ripple. Item VI calculates the value of the optimum zero sequence signal $v_{0\_ref\_OPT}$ that minimizes local RMS ripple value. It shows that the Space Vector PWM (SV_PWM) [3], which can be implemented by injecting a zero sequence signal $v_{0\_ref\_SV}$ to the four carrier based PWM blocks, has a behavior that is similar to the injection of $v_{0\_ref\_OPT}$. Item VI shows experimental results.

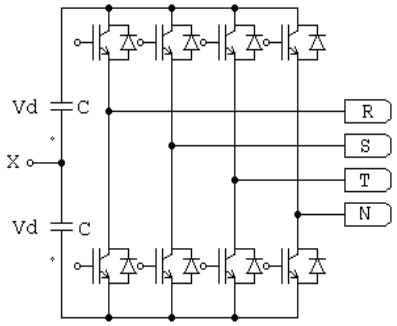


Figure 1. Voltage Source Converter/ 3-Phase / 4-Wire / Four Legs (VSC3P4W-FL)

## II. ANALISYS OF THE OUTPUT VOLTAGE RANGE

Figure 2 shows the locus of the vectors synthesized by a VSC3P4W-FL where the local average of the output voltages $v_{RX}; v_{SX}; v_{TX}$ vary in the range $\pm v_d$ and the local average of $v_{NX}$ is zero ($v_d = 1pu$). This figure shows the axes of the orthonormal basis $\alpha\beta 0$ and the axes of the basis $rst$. Figure 3 shows the space vector locus of the output voltage vector for $v_{NX}$ varying in the range $\pm v_d$. The voltage $v_{NX}$ displaces the original locus (figure 2) in the axis 0 direction, by a $\pm v_d$ amount. For a large range of $v_{NX}$ it is possible to achieve vectors whose $\alpha\beta$ coordinates lies inside the hexagon shown in figure 3. The increased output range is especially important for converters connected to the line, where the converter voltages must at least counteract the line voltages to impose zero current. Additionally, for example, in an active filter, high amplitude harmonic voltages

(balanced and zero sequence ones) must be injected.
The use of four independent PWM blocks or the Space Vector PWM enables the generation of any vector inside the external surface shown in figure 3.

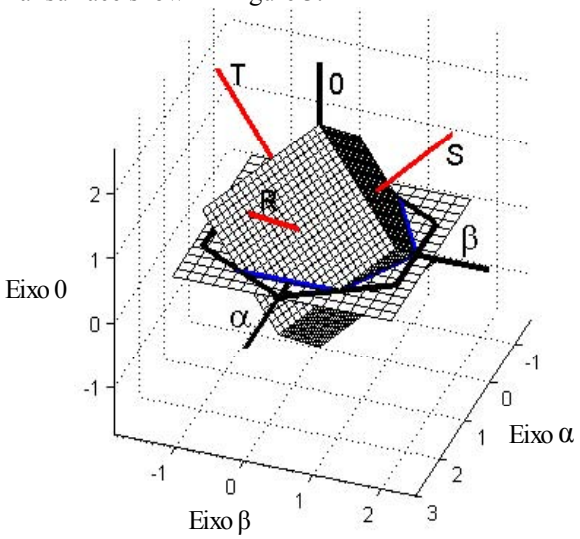


Figure 2. Locus of the vectors synthesized by a VSC3P4W-FL ( $v_{NX}$ =0)

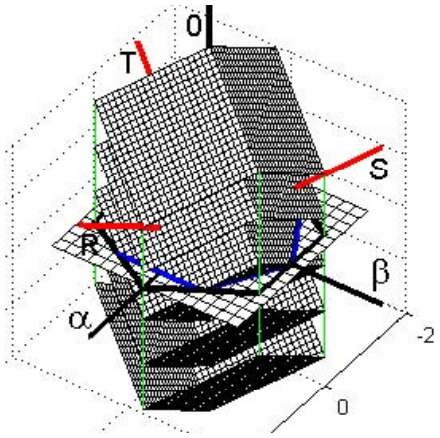


Figure 3. Locus of the vectors synthesized by a VSC3P4W-FL

## III. MODELING OF THE VSC3P4W-FL

The VSC3P4W-FL in figure 1 can be modeled as a Wye connection of four voltage-sources $v_{RX}; v_{SX}; v_{TX}, v_{NX}$ to the point X, according to figure 4. The load is modeled as a set of counter EMF [ $v_{CR}, v_{CS}, v_{CT}, v_{CN}$ ] satisfying the condition $v_{CR}+v_{CS}+v_{CT}=0$.

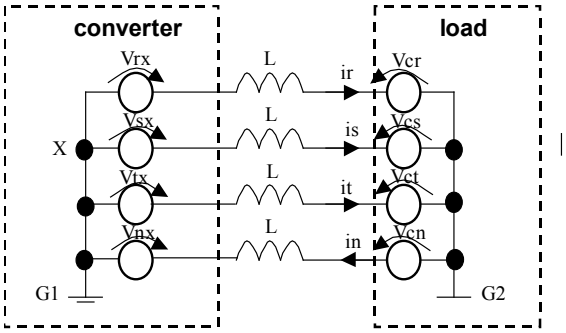


Figure 4. Model for the VSC3P4W-FL and its load

The set of converter voltages [ $v_{RX}; v_{SX}; v_{TX}$ ] contain the balanced ( $v_{Rb}\ v_{Sb}\ v_{Tb}$ ) and zero sequence ( $v_Z$ ) components defined by equations 1,2,3,4 using matrix notation. The sum of the balanced components is instantaneously equal to zero.

$$\mathbf{V} = \mathbf{V}_b + \mathbf{V}_{ZX} \tag{1}$$

$$\mathbf{V} = \left[v_{RX}; v_{SX}; v_{TX}\right]^t; \qquad \mathbf{V_{ZX}} = \left[v_Z\ v_Z\ v_Z\right]^t \tag{2}$$

$$\mathbf{V_b} = \left[v_{Rb}\ v_{Sb}\ v_{Tb}\right]^t = V - V_{ZX} \tag{3}$$

$$v_Z = (v_{RX} + v_{SX} + v_{TX})/3 \tag{4}$$

Using equations 1,2,3,4 and the "sources displacement theorem" results in the circuit shown in figure 5, where the balanced sequence components ( $v_{Rb}\ v_{Sb}\ v_{Tb}$ ) and the zero sequence component ( $v_Z$ ) are explicitly shown.

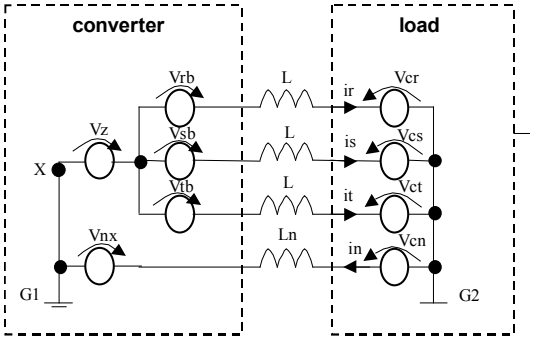


Fig 5. Zero Sequence Components de ( $v_Z$ , $v_{NX}$ ), and balanced components ( $v_{Rb}\ v_{Sb}\ v_{Tb}$ )

The zero and the balanced sequence components of the line current can be calculated by the superposition theorem.(equations 5, 6, 7).

$$L \cdot \frac{d\mathbf{I_b}}{dt} = \left(\mathbf{V_b} - \mathbf{V_C}\right) \tag{5}$$

where:

$$\mathbf{I_b} = \left[i_{Rb}\ i_{Sb}\ i_{Tb}\right]^t;\ \mathbf{V_C} = \left[v_{CR}\ v_{CS}\ v_{CT}\right]^t \tag{6}$$

$$\left(\frac{L}{3} + L_N\right) \cdot \frac{di_Z}{dt} = v_{ZX} + v_{CN} - v_{NX} \tag{7}$$

The line currents are obtained by the "Superposition Theorem" and presented in equation 8.

$$\begin{bmatrix} i_R \\ i_S \\ i_T \\ i_N \end{bmatrix} = \begin{bmatrix} i_{Rb} \\ i_{Sb} \\ i_{Tb} \\ 0 \end{bmatrix} + \begin{bmatrix} i_Z/3 \\ i_Z/3 \\ i_Z/3 \\ i_Z \end{bmatrix} \tag{8}$$

## IV. ANALYSIS OF THE INJECTION OF A ZERO SEQUENCE SIGNAL TO THE PWM REFERENCES

Figure 6 shows the waveforms of the reference signals $v_{RX\_ref}$, $v_{SX\_ref}$, $v_{TX\_ref}$, $v_{NX\_ref}$, the converter output voltages $v_{RX}; v_{SX}; v_{TX}, v_{NX}$ and the ripple at the line and neutral currents, for one switching cycle. The graphics at the right side column show the effect of injecting a zero sequence reference voltage to the four PWM blocks. For this particular case, current ripple reduction is achieved.
The behavior of the local average of the line and neutral currents is not altered. This fact can be explained by figure 5. If a signal $v_{0ref}$ is added to the four PWM references, it will appear simultaneously in the components $v_Z$ and $v_{NX}$, causing no changes in the behavior of the local average of the zero sequence currents (eq.7,8). However, the duty cycle of the PWM signals is changed, altering the local harmonic contents of the converter voltages and currents.
This can also be explained based on the space vectors generated by the converter. For the particular values of $v_{RX\_ref}$, $v_{SX\_ref}$, $v_{TX\_ref}$, $v_{NX\_ref}$ used in figure 6, the sequence of imposed space vectors is $\vec{V}_{15}$, $\vec{V}_{14}$, $\vec{V}_{12}$, $\vec{V}_8$, $\vec{V}_0, \vec{V}_8$, $\vec{V}_{12}$, $\vec{V}_{14}$, $\vec{V}_{15}$ (according to table I in appendix). Figure 6 shows that the injection of $v_{0ref}$ displaces vertically the four reference signals $v_{RX\_ref}$, $v_{SX\_ref}$, $v_{TX\_ref}$, $v_{NX\_ref}$. This equally displaces the transitions of the PWM signals $v_{RX}; v_{SX}; v_{TX}$ horizontally. Figure 6 shows that the time intervals of the active vectors $\vec{V}_{14}$, $\vec{V}_{12}$, $\vec{V}_8$ is not changed, resulting in the same average voltage vector for one switching period. The space vector sequence generated by the use of four PWM blocks and their vector duration is identical to the one used in the Space Vector PWM [1].

This reasoning suggests the possibility of searching an optimal value of $v_{0ref}$ that minimizes the ripple of the converter currents, which will be presented in the next item.
.

## V.OPTIMAL VALUE FOR THE ZERO SEQUENCE SIGNAL

The optimization problem consists to find an instantaneous value of $v_{0ref}$ ($v_{0ref} = v_{0ref\_opt}$) that minimizes the cost function ($i_{RMS}$) defined as the sum of the RMS values of the ripple currents for the line and neutral converter currents.
The constraints for the optimization problem are:
- use of VSC3P4W-FL converter with four identical filter inductors;
- use of regular symmetrical sampled PWM;
- use of the same carrier for the four PWM blocks;
- over modulation doesn't occur.

For a given quartet [$v_{RX\_ref}$ $v_{SX\_ref}$ $v_{TX\_ref}$ $v_{NX\_ref}$] of reference signals, and for a specific value of injected zero sequence reference $v_{0ref}$, the circuit is simulated using eqs. 5,7,8, and the cost function $i_{RMS}$ is evaluated. The injected signal $v_{0ref}$ is varied in a range that avoids over-modulation in any of the PWM blocks. The search of the minimal value of $i_{RMS}$ leads to the optimal injected zero sequence $v_{0ref\_opt}$. The curve $i_{RMS}$ x $v_{0ref}$ is well behaved, presenting one unique minimum point (fig 8).

To systematically sweep all the range of $v_{RX\_ref}$ $v_{SX\_ref}$ $v_{TX\_ref}$ $v_{NX\_ref}$ and evaluate $v_{0ref\_opt}$ for each set of reference signals:
- the trio $v_{RX\_ref}$ $v_{SX\_ref}$ $v_{TX\_ref}$ was choosen with the help of figure 7 that shows the projection of the Space Vector of the employed converter on the $\alpha\beta$ plane. The angle of the vector was varied in the range 0~360º and its amplitude in the range 0~1 $V_d$ (see fig 7). Each vector on $\alpha\beta$ plane defines a trio $v_{RX\_ref}$ $v_{SX\_ref}$ $v_{TX\_ref}$.

For each trio $v_{RX\_ref}$ $v_{SX\_ref}$ $v_{TX\_ref}$, the value of $v_{NX\_ref}$ is varied in the range ($-V_d \sim +V_d$)

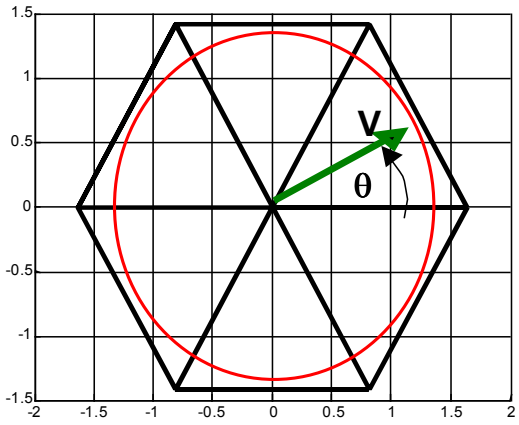

Figure 7 Choice of vectors on $\alpha\beta$ plane

Figure 8 shows the curves for $\theta = 30^o$ and V=1/3 $V_d$. Each curve corresponds to a value of $v_{NX\_ref}$ (see figure legend). The "+" symbol shows the minimum point. The complete set of graphics is not shown in this paper. This exhaustive method to evaluate $v_{0ref\_opt}$ is not suitable for practical applications. At this point, the some reasoning cited in [1,4,6,14] can be used. It states that the SVPWM can be obtained for a three-phase three-wire converter by injecting a zero sequence signal $v_{0ref}$. Paper [1,6,14] shows that $v_{0ref}$ is such as to make the time interval of the null vectors ($V_0$ and $V_7$) equal. This is equivalent to sum $v_{0ref}$ to force the maximum and minimum reference values to be equidistant to the zero. For the VSC3P4W-FL case, [1] states that for the SVPWM the time intervals of the null vectors $V_0$ and $V_{15}$ must be equal to minimize current ripple, without proof. According to figure 6 the sequence of the space vectors is identical for the Carrier PWM and SVPWM.

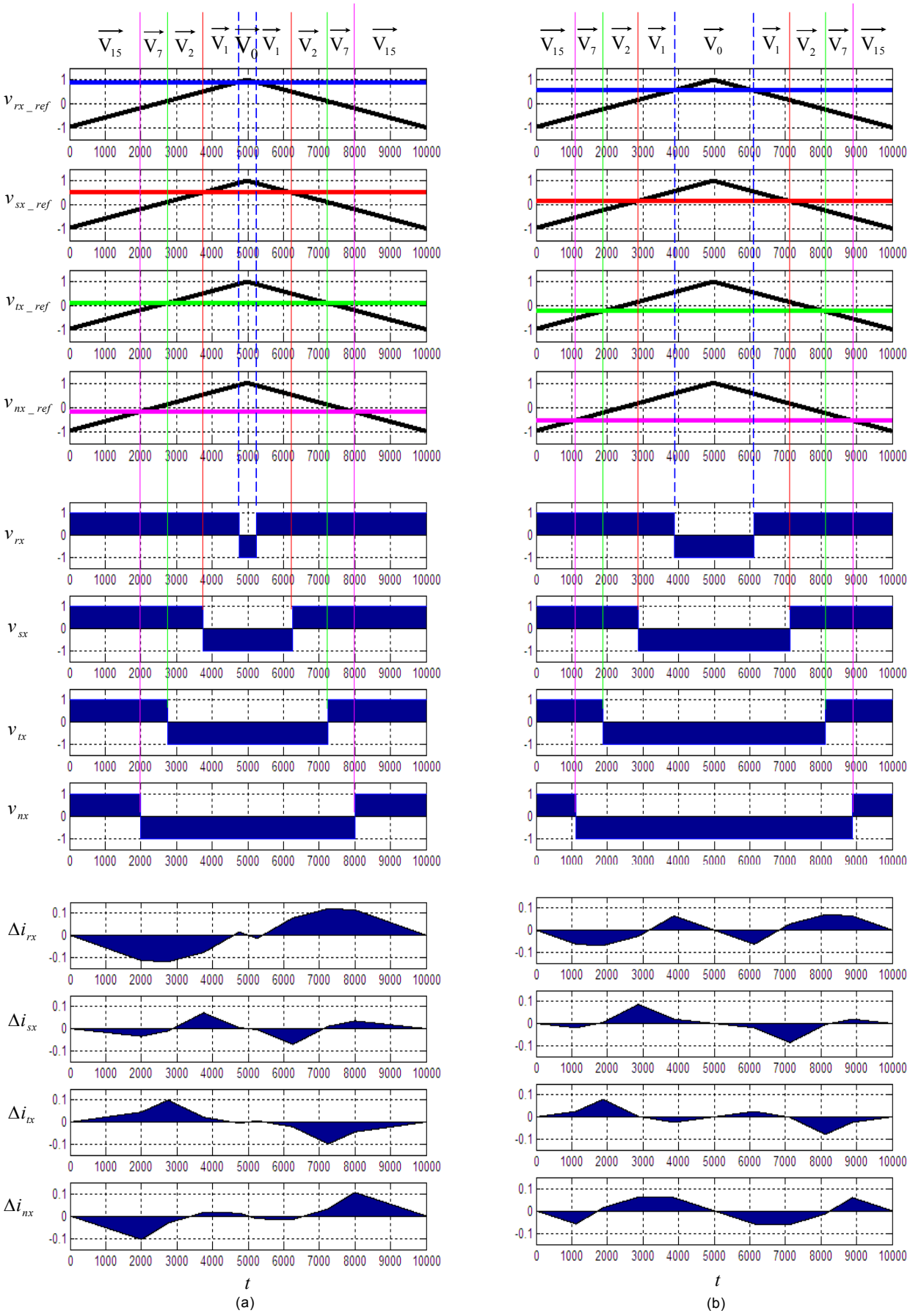


Figure 6. Simulated waveforms for a CPWM applied to a VSI3F4W-FL, showing one PWM cycle ( $T_S$ ): with arbitrary values of reference signals $v_{RX\_ref}(t)$, $v_{SX\_ref}(t)$, $v_{TX\_ref}(t)$ and $v_{NX\_ref}(t)$; Voltage Converters $v_{RX}(t)$, $v_{SX}(t)$, $v_{TX}(t)$ and $v_{NX}(t)$; and ripple current $\Delta i_r(t)$, $\Delta i_s(t)$, $\Delta i_t(t)$ and $\Delta i_n(t)$.
**Left: a)** $v_{0\_ref}(t) = 0$ . **Right: b)** $v_{0\_ref}(t) \neq 0$ (reference signals showed in blue, red, green and pink lines).

To force equal duration for $V_0$ and $V_{15}$, the maximum and minimum value of the set $[\,v_{RX\_ref}\;\; v_{SX\_ref}\;\; v_{TX\_ref}\;\; v_{NX\_ref}\,]$ must be equidistant. This is achieved by injecting $v_{0ref\_SV}$ defined in equation. 9

$$v_{0\_ref\_SV} = -\frac{\max(\mathbf{V_{ref}}) + \min(\mathbf{V_{ref}})}{2} \qquad (9)$$

$$where: \quad \mathbf{V_{ref}} = [v_{RX\_ref}; v_{SX\_ref}; v_{TX\_ref}; v_{NX\_ref}]$$

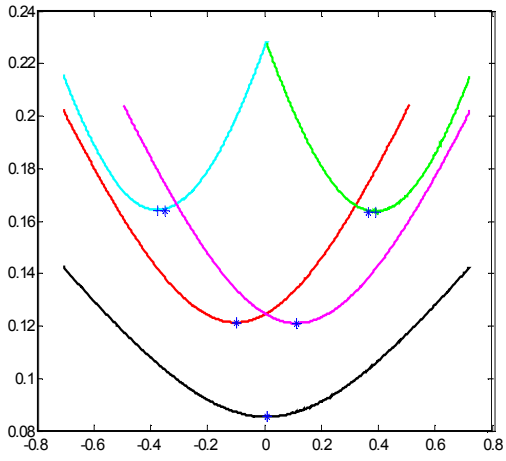

Figure 8 Plots of $i_{RMS}$ x $v_{0ref}$ for $\theta = 30^o$ and V=1/3 $V_d$ ; for: ( $v_{NX\_ref}$ = -1.0 $V_d$ (green), -0.5 $V_d$ (magenta), 0 (black), 0.5 $V_d$ (red) , 1.0 $V_d$ (cyan)

To verify the optimality of the SVPWM and the carrier PWM (CPWM) with injection of $v_{0ref\_SV}$, the value of $i_{RMS}$ was calculated for all of the previously simulated cases and shown in figure 8 by a "*" symbol. It shows the quasi-optimum behavior of the SVPWM and the CPWM with injection of $v_{0ref\_SV}$. The signal $v_{0ref\_SV}$ evaluated by using eq.9 is easy to calculate. The carrier based PWM is included in all "power electronics" dedicated CPUs, requiring no extra processing. This makes this solution preferable when compared to the SVPWM implementation.

## VI. EXPERIMENTAL RESULTS

A prototype of a VSC3F4W-FL using IGBTs and controlled by an DSP TMS320LF2407A was implemented (figure 9). Experimental results are shown considering:
$2V_d$ = 37.5V, R = 24Ω, C=10µF, L = 20mH, LN = 25mH.
Experimental results are shown in per unit values. The currents were measured, their fundamental component evaluated and used to calculate the ripple current (figure 10, 11). The measured currents were numerically processed using Matlab to extract their fundamental components, and to obtain only the ripple currents.

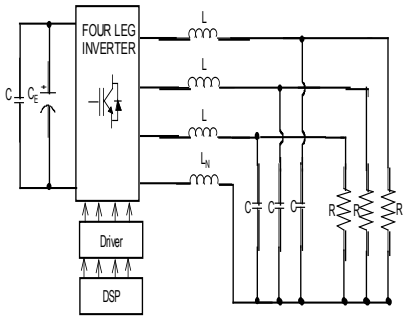


Figure 9. Experimental setup for the VSI3F4W-FL

Figure 10 presents the ripple at the line and neutral conductor and their spectra for the case with $v_{0ref}$ =0.
In figure 11 $v_{0ref} = v_{0ref\_SV}$ is injected, showing a good improvement in the ripple amplitude.

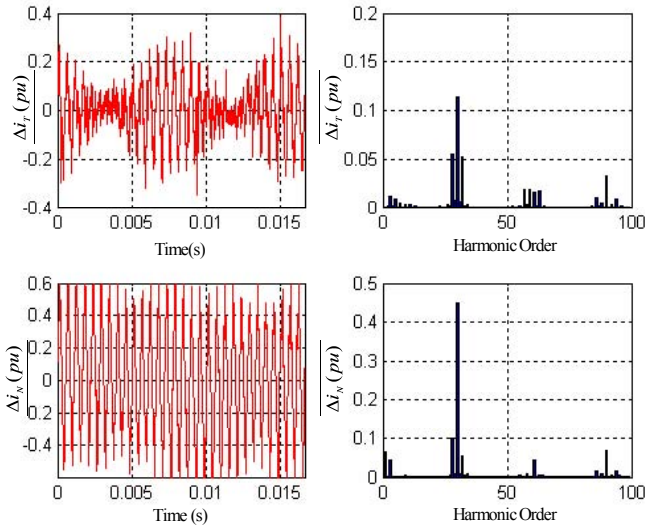


Figure 10 Experimental Results – Ripple current and their spectral for **no injection of zero sequence** $v_{0ref} = 0$. Top (line current) and Botton (neutral current)

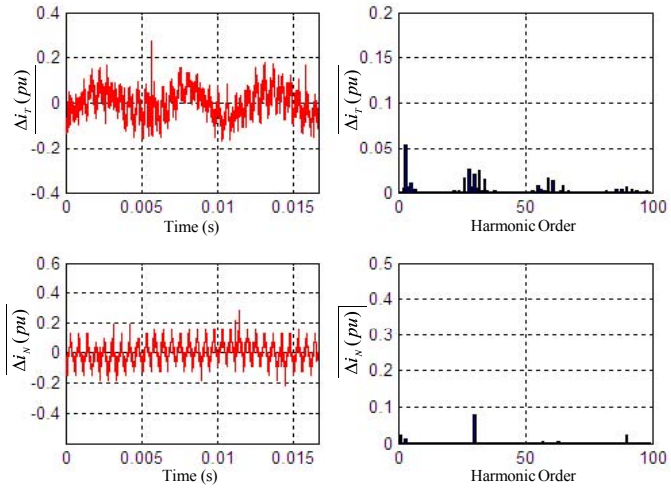


Figure 11 Experimental Results – Ripple current and their spectral for **injection quasi-optimal of zero sequence** $v_{0ref} = v_{0ref\_SV}$. Top (line current) and Botton (neutral current)

## VII. CONCLUSION

The implementation of the SVPWM for the VSC3F4W-FL converter by zero sequence injection in a conventional carrier based PWM is discussed. An optimum value for the injected zero sequence signal which minimizes the sum or the RMS values of the ripple currents is evaluated. The quasi-optimum behavior of the SVPWM for minimizing current ripple is emphasized. A simple formula for on line evaluation of the injected zero sequence is shown. Considering that the Carrier PWM requires no additional computational load in the commercially available DSPs, the discussed PWM is an attractive option for implementing four wire- three-phase converters.

## REFERENCES

[1] Bowes S.R. and Lay Y.S., The Relationship Between Space Vector Modulation and Regular Sampled PWM. IEEE Transaction on Power Electronics, Vol. 44, No. 5, pp. 670-679, 1997.

[2] H. Pinheiro et. Al, "Modulação Space Vector para Inversores Alimentados em Tensão : Uma Abordagem Unificada", XIV Congresso Brasileiro de Automática (CBA), 2002, pp. 787-794.

[3] Pinheiro H. et. Al; Novos Algoritmos de Limitação para Inversores de Tensão PWM a Quatro Braços utilizando Modulação Space Vector; Revista Controle & Automação, vol.15 no. 3, Julho-Agosto-Setembro 2004

[4] Joaquim Holtz, "Pulsewidth Modulation - A Survey", IEEE Transactions on Industrial Electronics, Vol. 39, No. 5, September 1985.

[5] Juang-Hwan King and Seung-Ki Sul, "A Carrier-Based PWM Method for Three-Phase Four-Wire Voltage Source Converters", Transactions on Power Electronics, Vol. 19, No. 1, January 2004, pp. 66-75.

[6] Matakas Jr. L. and Komatsu K, "A Didactic Comparison of Space-Vector PWM and Carrier-Based PWM with Optimal Zero-Sequence Injection"; COBEP2005, Recife, Brazil.

[7] Matakas Jr. L. et al., "Instantaneous Optimum PWM and its comparison to the Space Vector and regular Sampling Methods", Nat. Conv. IEEE, Japan 1994.

[8] Michael J. Ryan, Robert D. Lorenz and Rick W. De Doncker, "Modeling of Multileg Sine-Wave Inverters: A Geometric Approach", Transactions on Industrial Electronics, Vol. 46, No. 6, December 1999, pp. 1183-1191.

[9] Nguyen-Van Nho, Myung B. Kim, Gun W. Moon and Myung J. Youn, "A Novel Carrier Based PWM Method in Three Phase Four Wire Inverters", Transactions on Power Electronics, November 2004.

[10] S.M. Ali and M.P. Kasmierkowshi, "PWM Voltage and Current Control of Four-Leg VSI", IEEE Transaction on Power Electronics, 1998, pp. 196-201.

[11] S.M. Ali and M.P. Kasmierkowshi, "Current Control Techniques for Three-Phase Voltage-Source PWM Converters: A Survey", IEEE Transaction on Industrial Electronics, Vol. 45, No. 5, October 1998, pp. 691-703.

[12] Villalva M.G. et. Al., "Detailed Implementation of a Current Controller with 3D Space Vector for Wire Active Filters", IEEE Transaction on Industrial Electronics, Vol. 32, No. 6, October 2003, pp. 536-541.

[13] Walter P. Silva Jr., Matakas Jr. L. and Antonio R. Giaretta, "Comparing Two Strategies for the Implementation of Three-Phase Four-Wire VSI Converters", Induscon 2006, April 2006, Recife, Brazil.

[14] Keliang Zhou, Danwei Wang, "Relationship Between Space Vector Modulation and Three-Phase Carrier Based PWM: A Comprehensive Analysis", IEEE Trans. On Industrial Electronics, Vol 49, No.1 february 2002, 186-196

## APPENDIX A: TABLE OF SPACE VECTORS

**TABLE 1**
Definition of the Space Vectors

| $V_{RX}$ | $V_{SX}$ | $V_{TX}$ | $V_{NX}$ | SV |
|---|---|---|---|---|
| $-V_d$ | $-V_d$ | $-V_d$ | $-V_d$ | $\vec{V}_0$ |
| $V_d$ | $-V_d$ | $-V_d$ | $-V_d$ | $\vec{V}_1$ |
| $-V_d$ | $V_d$ | $-V_d$ | $-V_d$ | $\vec{V}_2$ |
| $V_d$ | $V_d$ | $-V_d$ | $-V_d$ | $\vec{V}_3$ |
| $-V_d$ | $-V_d$ | $V_d$ | $-V_d$ | $\vec{V}_4$ |
| $V_d$ | $-V_d$ | $V_d$ | $-V_d$ | $\vec{V}_5$ |
| $-V_d$ | $V_d$ | $V_d$ | $-V_d$ | $\vec{V}_6$ |
| $V_d$ | $V_d$ | $V_d$ | $-V_d$ | $\vec{V}_7$ |
| $-V_d$ | $-V_d$ | $-V_d$ | $V_d$ | $\vec{V}_8$ |
| $V_d$ | $-V_d$ | $-V_d$ | $V_d$ | $\vec{V}_9$ |
| $-V_d$ | $V_d$ | $-V_d$ | $V_d$ | $\vec{V}_{10}$ |
| $V_d$ | $V_d$ | $-V_d$ | $V_d$ | $\vec{V}_{11}$ |
| $-V_d$ | $-V_d$ | $V_d$ | $V_d$ | $\vec{V}_{12}$ |
| $V_d$ | $-V_d$ | $V_d$ | $V_d$ | $\vec{V}_{13}$ |
| $-V_d$ | $V_d$ | $V_d$ | $V_d$ | $\vec{V}_{14}$ |
| $V_d$ | $V_d$ | $V_d$ | $V_d$ | $\vec{V}_{15}$ |